09.1

Anomalous fast luminescence of $CsCeSiS_4$ thiosilicate

© V.A. Pustovarov[1], D.A. Tavrunov[1], M.S. Tarasenko[2], N.G. Naumov[2]

[1] Ural Federal University after the first President of Russia B.N. Yeltsin, Yekaterinburg, Russia
[2] Nikolaev Institute of Inorganic Chemistry, Siberian Branch of Russian Academy of Sciences, Novosibirsk, Russia
E-mail: v.a.pustovarov@urfu.ru

Received August 30, 2023
Revised November 1, 2023
Accepted November 2, 2023

$CsCeSiS_4$ thiosilicate single crystals were obtained by high-temperature flux synthesis. The absorption spectrum in the region of 450 nm is formed by $f \rightarrow d$ transitions in the Ce^{3+} ion. The nonelementary $5d \rightarrow 4f$ band of Ce^{3+} ion emission is observed in the photo- and X-ray excited luminescence spectra in the region of 520 nm at temperatures of 5−330 K. The inertialess luminescence decay kinetics upon excitation by X-ray synchrotron radiation is characterized by a dominant component with a decay time $\tau = 0.88$ ns. The luminescence of Ce^{3+} ions is efficiently excited by the intracenter way or due to the recombination of band charge carriers.

Keywords: Ce^{3+} ion, luminescence decay kinetics, interconfigurational transitions, synchrotron radiation.

DOI: 10.61011/PJTF.2024.03.57035.19714

For the tasks of radiation monitoring, nuclear medicine, computer diagnostics the search for new materials — fast and effective converters of various types of ionizing radiation is relevant. Inorganic dielectrics or wide-gap semiconductors, which exhibit cross-luminescence [1], intraband luminescence [2], luminescence of unrelaxed excitons [3], or interconfiguration $d-f$-rare-earth ion (REI) luminescence, are suitable for this purpose. The materials doped with Pr^{3+}, Ce^{3+}, Eu^{2+} ions are characterized by the highest light yield and nanosecond luminescence decay kinetics. It is these dopant ions that are used in modern scintillation materials [4–9].

Sulfide-based luminescent materials have attracted attention because of their efficient broadband emission, which finds application in the development of LEDs of different spectral composition [10]. In addition, the applications of sulfides are flat displays using thin-film electroluminescence, emission displays, particularly ZnS-based displays. The doping of sulfides with Ce^{3+} or Eu^{2+} ions allows us to consider them as promising fast converters of various kinds of radiation [10,11].

Among sulfide-based materials, the class of thiosilicates can be distinguished (see, e.g., [11–13]). The prefix „thio" means replacing oxygen with sulfur. This class of compounds has been studied very superficially, the main focus has been on the study of crystal structure and nonlinear optical properties. In the present work, single crystals of $CsCeSiS_4$ are studied by absorption spectroscopy and by photoluminescence spectroscopy within the temperature range of 5−330 K. Pulsed synchrotron radiation of X-ray range is used for spectral-kinetic studies.

The crystals were synthesized by the method described in [12,14], and were yellowish plates a few millimeters in size. X-ray diffraction analysis showed that the diffractograms show reflections exclusively corresponding to the crystal structure of $CsLaSiS_4$ in the orthorhombic spatial group $Pnma$, with no traces of other phases (see for details [14]). The crystal lattice parameters of the synthesized $CsCeSiS_4$ are as follows: $a = 17.852(2)$ Å, $b = 6.732(1)$ Å, $c = 6.460\,(1)$ Å, volume of lattice cell is 776.36 Å^3, number of formula units in the lattice cell is $z = 4$, calculated density is 3.67 g/cm^3. Effective atomic number $Z_{eff} = 53$.

Absorption spectra were registered on a Helios-Alpha spectrophotometer. Photoluminescence (PL) spectra were measured on a HORIBA iXR320 Fluorolog spectrometer using the method described in [14]. X-ray luminescence (XRL) spectra and decay kinetics were measured in the synchrotron radiation (SR) channel № 6 on the VEPP-3 storage ring at the G.I. Budker Institute of Nuclear Physics, Siberian Branch of the Russian Academy of Sciences. SR- pulse parameters: energy 3−60 keV, pulse time (FWHM) ∼ 1 ns, frequency 8 MHz. The stroboscopic method of electron-optical chronography with subnanosecond temporal resolution using the LI-602 dissector was applied. The PL and XRL spectra presented in this work are corrected for the spectral sensitivity of the detection system.

The absorption spectrum of $CsCeSiS_4$ is shown in Fig. 1, *a*. The absorption spectrum of the low cerium content crystal $CsLa_{1-x}Se_xSiS_4$ ($x = 0.005$) is also shown for comparison. The crystal with low cerium concentration is transparent in the 350−800 nm region, and the absorbance is minimal and does not exceed 0.5. A sharp increase in the absorbance is observed at wavelengths below 340 nm, with only a weak shoulder visible in the 340−400 nm region. On the contrary, in $CsCeSiS_4$, a sharp increase in absorbance is observed already at 450 nm, which determines the yellowish color of the crystal. In the work [14], the interband transition energy $E_g = 3.75$ eV was determined using the Tauc method in the study of $CsLaSiS_4$ doped with Ce^{3+} ions. It follows from the comparison that the sharp increase in absorbance in $CsCeSiS_4$ in the 450 nm region is due to the electronic transitions $4f \rightarrow 5d$ in the Ce^{3+} ion.

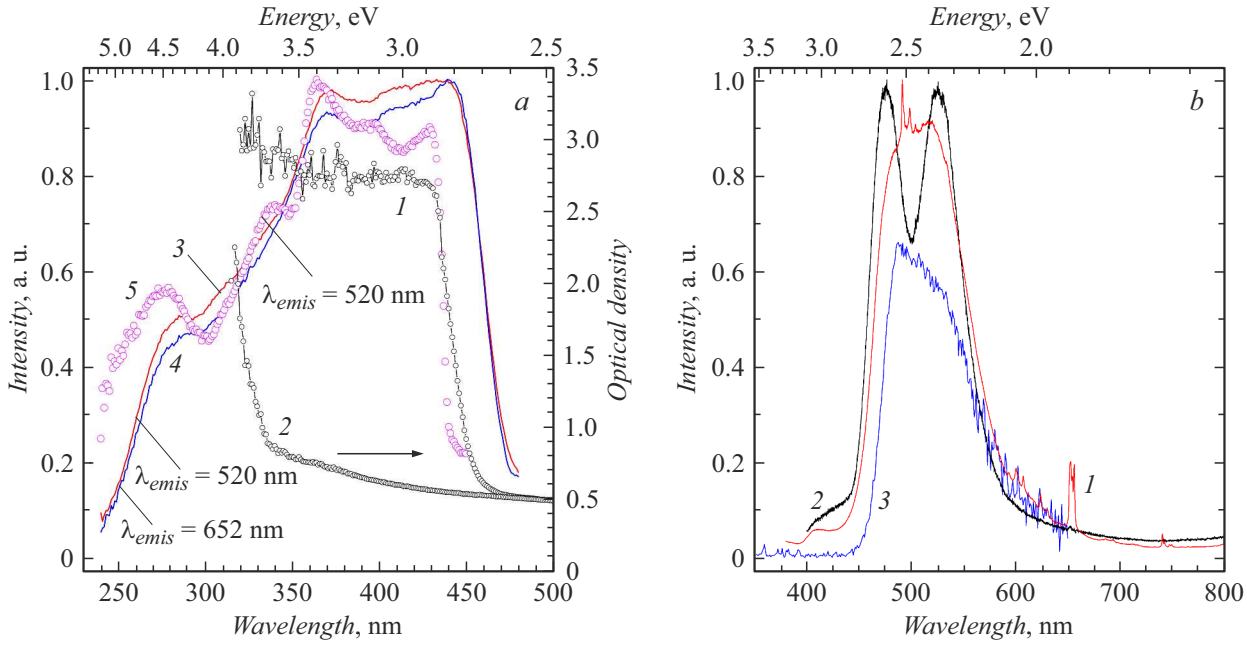

Figure 1. *a* — absorption spectra of crystals $CsCeSiS_4$ (*1*) and $CsLa_{1-x}Ce_xSiS_4$ ($x = 0.005$) (*2*) at $T = 295$ K and PL excitation spectra $CsCeSiS_4$ for various emission bands at $T = 295$ (*3*, *4*) and 5 K (*5*); *b* — PL spectra of $CsCeSiS_4$ at $T = 295$ (*1*) and 5 K (*2*) ($\lambda_{exc} = 280$ nm) and XRL at $T = 295$ K (*3*).

Fig. 1, *b* shows the normalized PL spectra of $CsCeSiS_4$ under excitation by photons with wavelength $\lambda_{exc} = 280$ nm at different temperatures and the XRL spectrum. At $T = 295$ K, a broad non-elementary band in the region of 520 nm is observed in the PL spectra; the position and shape of this band remain unchanged irrespective of the excitation photon energy in the range of 250–450 nm. In its background, as well as in the 600–650 nm region, weak narrow lines $f-f$- of transitions in uncontrolled REI impurity, probably present in the precursors, are observed. At = 5 K in the PL spectrum, the non-elementary band splits into two components: 475 and 525 nm, which correspond to emission transitions from the lowest excited 5*d*-level to two sublevels of the spin-orbitally split ground $4f$-state $^2D_{3/2} \rightarrow {}^2F_{5/2}$ and $^2D_{3/2} \rightarrow {}^2F_{7/2}$ in Ce^{3+} ions.

The photoluminescence excitation (PLE) spectra of $CsCeSiS_4$ for different emission bands at $T = 295$ and 5 K compared to the absorption spectra are shown in Fig. 1, *a*. In PLE spectra, a group of bands in the range 310–440 nm is observed, which falls both in the crystal transparency region $CsLa_{1-x}Se_xSiS_4$ ($x = 0.005$) and in the absorption region $CsCeSiS_4$. It follows that this group of bands corresponds to electronic transitions from the ground $4f$-state to different sublevels of the excited 5*d*- configuration $^2F_{5/2,7/2} \rightarrow {}^2D_{3/2,5/2}$ in Ce^{3+} ions. The broad short-wavelength band below 310 nm in the PLE spectra corresponds to the fundamental absorption edge and the region of interband transitions of the crystal $CsLaSiS_4$ [14], i.e. excitation of Ce^{3+} ion emission in $CsCeSiS_4$ can occur both by intracenter pathway and due to recombination of band charge carriers on Ce^{3+} centers. The high XRL yield (Fig. 1, *b*) confirms the efficiency of the recombination channel for excitation of Ce^{3+} luminescence. Further, the coincidence of the excitation spectrum of the 520 nm band corresponding to the transition $^2D_{3/2} \rightarrow {}^2F_{7/2}$ in Ce^{3+} and the excitation spectrum of the 652 nm line corresponding to $f-f$- emission of an uncontrolled REI impurity indicates a resonant emission mechanism of energy transfer $Ce^{3+} \rightarrow$ REI.

Fig. 2 shows the PL spectra of $CsCeSiS_4$ at different temperatures (*a*) and the temperature dependence of the integral (in the range 450–650 nm) PL yield of the centers of Ce^{3+} (*b*). The measurements were carried out at the excitation photon wavelength $\lambda_{exc} = 300$ nm, corresponding to the creation of band charge carriers in $CsCeSiS_4$. It is seen that with increasing temperature from 5 K the splitting of the ground state terms $^2F_{5/2}$ and $^2F_{7/2}$ ceases to appear from- because of the temperature broadening of both bands. The temperature dependence of the PL yield does not obey the classical Mott formula for intracenter quenching and can be characterized by the temperature $T_q = 160$ K, at which the PL yield is halved. This is determined by the fact that at the interband excitation $\lambda_{exc} = 300$ nm, the PL yield is due not only to intracenter quenching, but also to the probability of capture and recombination of band charge carriers at the impurity center.

The kinetics of the $CsCeSiS_4$ XRL decay in the 520 nm band is shown in Fig. 3, *a*. It can be seen that it differs only slightly from the excitation SR--pulse profile, and it should be noted that there is no scattered light in the X-ray SR- excitation. The parameters of the XRL decay kinetics were determined under the assumption that the experimental decay curve is a convolution of the excitation

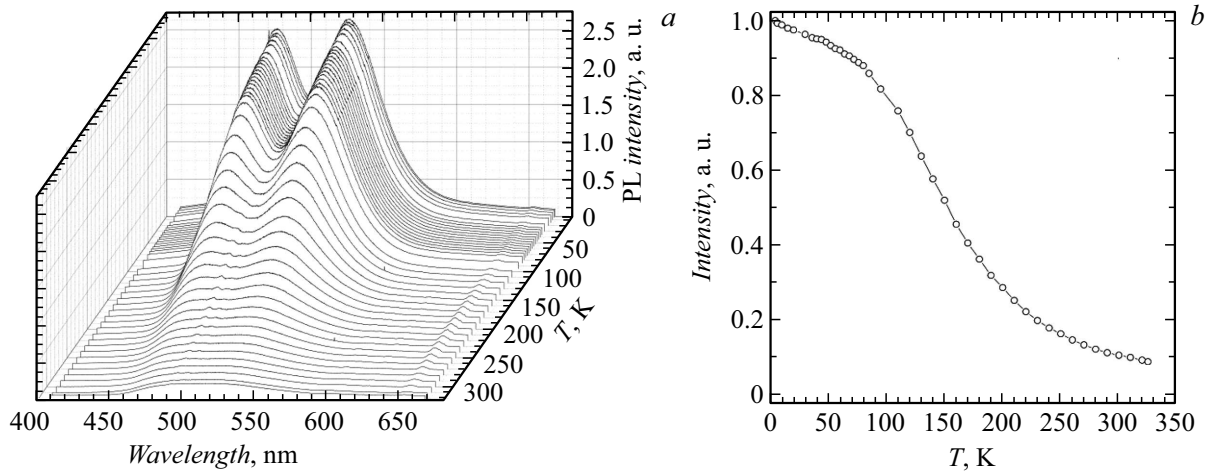

Figure 2. *a* — PL spectra of $CsCeSiS_4$ at different temperatures ($\lambda_{exc} = 300$ nm); *b* —temperature dependence of the integrated yield of PL of Ce^{3+} centers.

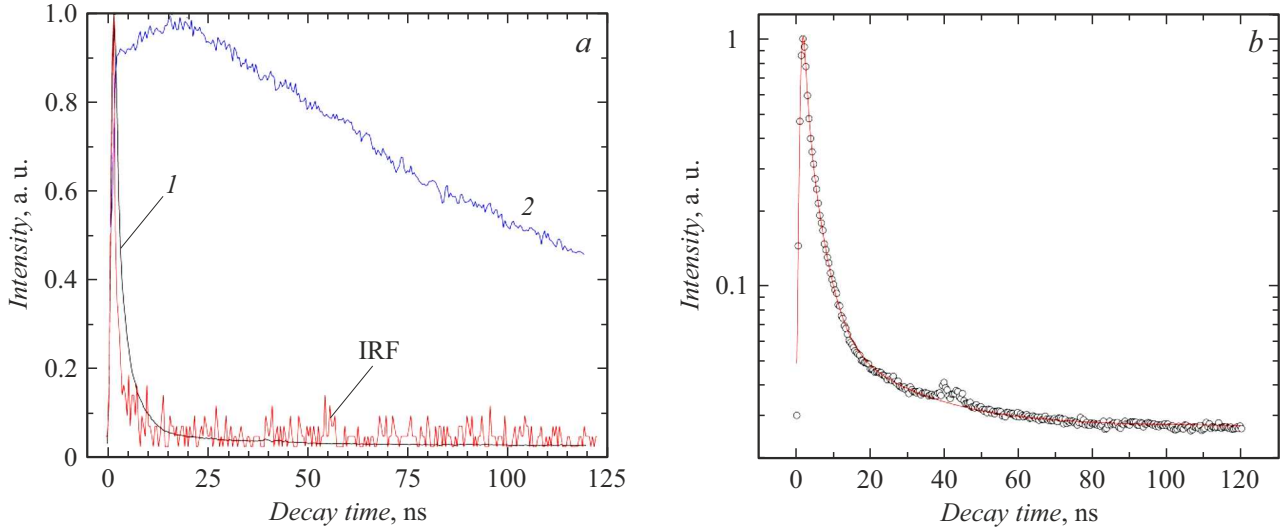

Figure 3. *a* — Decay kinetics of XRL of $CsCeSiS_4$ (1) and $CsLa_{1-x}$ $CexSiS_4$ ($x = 0.005$) (2) at the 520 nm emission band, $T = 95$ K, IRF — profile of excitation SR-pulse; *b* — Decay kinetics of XRL of $CsCeSiS_4$ (dots) and its approximation by convolution calculation (line).

function (the excitation pulse has a Gaussian shape with the parameter $\sigma = 0.49$ ns) and the fluorescence function. The exponential decay kinetics and its parameters were determined from the best coincidence of experimental data and convolution calculation. The best correlation was achieved using a double-exponential XRL decay curve with parameters $\tau_1 = 0.88 \pm 0.04$ ns, $\tau_2 = 3.4 \pm 0.1$ ns, component amplitude ratio $A_1/A_2 = 2.12/1$. Fig. 3, *b* shows the result of approximation by convolution calculation.

The decay time of the dominant component $\tau_1 = 0.88$ ns is anomalously small relative to the typical decay time of radioluminescence of Ce ions^{3+} in various matrices, which is 30–60 ns or more, and depends on the concentration of impurity centers [4,8,9]. It can be assumed that in $CsCeSiS_4$ this is due to concentration quenching: the interaction of close centers of Cs^{3+} shortens the lifetime of electrons in the excited emission state $^2D_{3/2}$ [9]. To confirm this, the XRL kinetics of the crystal $CsLa_{1-x}Ce_xSiS_4$ ($x = 0.005$) with low concentration of Ce^{3+} ions are also shown in Fig. 3, *a*. The kinetics is characterized by a buildup stage (16 ns) and a much longer decay time (132 ns). The presence of buildup indicates the intermediate localization of charge carriers on small traps and reflects the processes of migration of electronic excitations in the crystal lattice.

Acknowledgments

In the experiments using synchrotron radiation, the equipment of the Center for Collective Use „Siberian Center of Synchrotron and Terahertz Radiation“ on the basis of

a unique research installation „VEPP Complex-4−VEPP-2000“ at the G.I. Budker Institute of Nuclear Physics of the Siberian Branch of the Russian Academy of Sciences was used.

Funding

This work was partially supported by the Ministry of Science and Higher Education of the Russian Federation (projects № FEUZ-2023-0013 and 121031700315-2) and the Strategic Academic Leadership Program „Priority-2030“ of the Ural Federal University.

Conflict of interest

The authors declare that they have no conflict of interest.

References

[1] Yu.M. Alexandrov, V.N. Makhov, T.I. Syreyshchikova, P.A. Rodny, M.N. Yakimenko, FTT, **26** (9), 2865 (1984).
[2] S.I. Omelkov, V. Nagirnyi, S. Gundacker, D.A. Spassky, E. Auffray, P. Lecoq, M. Kirm, J. Lumin., **198**, 260 (2018). DOI: 10.1016/j.jlumin.2018.02.027
[3] I.D. Venevtsev, A.E. Muslimov, Tech. Phys. Lett., **49** (9), 30 (2023). DOI: 10.61011/TPL.2023.09.56704.19641.
[4] J. Glodo, W.W. Moses, W.M. Higgins, E.V.D. van Loef, P. Wong, S.E. Derenzo, M.J. Weber, K. Shah, IEEE Trans. Nucl. Sci., **52**, 1805 (2005). DOI: 10.1109/TNS.2005.856906
[5] A.M. Srivastava, J. Lumin., **169** (B), 445 (2016). DOI: 10.1016/j.jlumin.2015.07.001
[6] A. Zych, M. de Lange, C. de Mello Donegá, A. Meijerink, J Appl. Phys., **112** (1), 013536 (2012). DOI: 10.1063/1.4731735
[7] V.A. Pustovarov, I.N. Ogorodnikov, A.A. Goloshumova, L.I. Isaenko, A.P. Yelisseyev, Opt. Mater., **34** (5), 926 (2012). DOI: 10.1016/j.optmat.2011.12.012
[8] P. Lecoq, A. Gektin, M. Korzhik, *Inorganic scintillators for detector systems* (Springer, Cham, 2017). DOI: 10.1007/978-3-319-45522-8
[9] C.W.E. van Eijk, J. Andriessen, P. Dorenbos, R. Visser, Nucl. Instr. Meth. A, **348** (2-3), 546 (1994). DOI: 10.1016/0168-9002(94)90798-6
[10] P.F. Smet, I. Moreels, Z. Hens, D. Poelman, Materials, **3** (4), 2834 (2010). DOI: 10.3390/ma3042834
[11] Y. Nanai, H. Kamioka, T. Okuno, J. Phys. D: Appl. Phys., **51** (13), 135103 (2018). DOI: 10.1088/1361-6463/aaaf5e
[12] M.S. Tarasenko, R.V. Duritsyn, D.A. Potapov, N.V. Kuratieva, A.A. Ryadun, N.G. Naumov, J. Struct. Chem., **63** (12), 1988 (2022). DOI: 10.1134/S0022476622120101.
[13] M. Usman, M.D. Smith, G. Morrison, V.V. Klepov, W. Zhang, P.S. Halasyamani, H.-C. zur Loye, Inorg. Chem., **58** (13), 8541 (2019). DOI: 10.1021/acs.inorgchem.9b00849
[14] V.A. Pustovarov, M.S. Tarasenko, D.A. Tavrunov, N.G. Naumov, J. Lumin., **265**, 120229 (2024). DOI: 10.1016/j.jlumin.2023.120229

Translated by D.Kondaurov